Proceedings of the 2nd National Aero Propulsion Conference
NAPC-2018
Dec 17-19, 2018, IIT Kharagpur, West Bengal

Submission No.:99

Characteristic Study of stationary flames using Flat flame Burner

Meghasham Khandige
Indian Institute of Space Science & Technology
Trivandrum, Kerala

Karthikeyan Rajasekar
Indian Institute of Technology
Madras, Tamil Nadu

Shrey Waghmare
Indian Institute of Space Science & Technology
Trivandrum, Kerala

Prof. S. R. Chakravarthy
Indian Institute of Technology
Madras, Tamil Nadu

Aritra Chakraborty
Indian Institute of Technology
Madras, Tamil Nadu

Dr. Prathap C
Indian Institute of Space Science & Technology
Trivandrum, Kerala

ABSTRACT

The objective of the present work was to design, fabricate and characterize a flat flame burner which anchors planar laminar premixed flames. To calibrate the burner, premixed methane-air flame was anchored and its Laminar Burning Velocity (LBV) was measured at near adiabatic condition. Then the flow field at the exit of the burner was measured using planar particle image velocimetry at both cold and reactive flow conditions. Flat flame burner was designed according to literature and fabricated. It consisted of a custom drilled perforated plate of 1611 holes with a diameter of 0.5mm. K-type thermocouples with a bead diameter of 0.25mm were used to measure the radial temperature distribution of burner plate. Burner was provided with a constant flow rate of premixed methane-air mixture at known equivalence ratio at 300K. A planar flame was anchored. From the information of reactant flow rate and flame across sectional area, LBV was estimated. LBV of 35.7±0.22cm/s was measured for premixed methane-air mixture which exactly matched with literature data. This validated the functioning of the newly constructed flat flame burner.

Also, in the present work, velocity field at the exit of the burner was also measured using PIV. Dual pulsed Nd: YAG Laser, light sheet optics and CCD Camera were used to track the seeder particles in a plane and to record the Mie scattered information. Zirconium Dioxide solid seeding particles were used. Acquired images were post processed using commercial PIV Software. Experiments were conducted for a mean unburned gas velocity of 25cm/s, 35cm/s and 40cm/s at Φ=0.8,1.0 and 1.3 at both isothermal and reacting flow conditions. Axial and radial velocity distribution at the exit of the burner were measured with the help of PIV.

NOMENCLATURE

Symbols	Description
S_L	Laminar burning velocity
U_g	Unburned gas mixture
Φ	Equivalence ratio

INTRODUCTION

Combustion processes are characterized by the complex interaction between different transport processes and numerous chemical reactions. To study the processes and to validate numerical calculations, non-intrusive techniques are necessary. In this work, a 1-D flame was used which allow us to measure its characteristics with less complication. In this pursuit, Particle Image Velocimetry (PIV) was used to measure the planar velocity distribution at the exit of the flat flame burner for both cold and reacting flow conditions. Planar Laser Induced fluorescence (PLIF) is normally used to excite and measure the emissions from OH in the combustion zone at high spatial and temporal resolution [1]. With proper calibration, the OH emission intensity can be converted into mole fraction of OH in the combustion zone. One of the common methods for calibration of OH PLIF is UV Absorption spectroscopy [2].

As mentioned above, PIV Measurements were applied to a planar stationary flame anchored using flat flame burner because of its simplicity and accuracy involved in the estimation of desired characteristics. In order to calibrate the burner, one of the most important parameters of fuel+ oxidizer mixture, i.e., the laminar burning velocity, S_L is estimated by performing validation experiments. It is an important parameter characterizing the propagation and stabilization of premixed flames, defined for freely propagating planar flame under adiabatic and steady conditions. S_L is a property of a fuel+ oxidizer mixture that depends on the gas mixture composition, Φ, unburnt gas temperature

and pressure. There are several methods to determine S_L. One of the most suitable methods is the Heat Flux Method as it involves planar flames [3].

The idea of measuring Laminar Burning Velocity by determining heat loss necessary for stabilizing the flame by measuring the temperature increase of water used for cooling the burner was originally put forwarded by Botha, J, P., Spalding, D, B [4]. Due to practical problems, Prof. De Goey and his co-workers improved and published the most accurate method to determine LBV by Heat Flux Method. The detail of burner design and typical methods were mentioned in their works [5][6]. A detailed description of different causes of uncertainties involved in the Heat Flux Method and the methodologies to improve the accuracy in the measurement of Laminar Burning Velocity was contributed by Vladimir Alekseev., et., al. [7].

HEAT FLUX METHOD

In this method, a planar flame is anchored at the exit of a perforated burner plate. Burner plate was maintained at a temperature above than that of the unburned gases. The basic idea behind keeping the burner plate at higher temperature than unburned gases is to compensate the thermal energy loss by the flame to the plate with thermal energy gain of unburned gases when they flow through the hot burner plate. This compensation of thermal energy loss by flame to the burner plate will allow stabilizing a near adiabatic flame at the exit of flat flame burner and this method is called Heat Flux Method. Fig.2 shows the layout of flat flame burner with temperature control that was employed in the Heat Flux Method. Prof. De Goey and his co-workers devised a certain mechanism to heat the burner plate at temperature higher than the unburned gases to facilitate thermal energy gain by unburned gases. Several K-type thermocouples (bead diameter 0.25mm) were used to measure the temperature of the burner plate to quantify the compensation of thermal energy.

Generally, the measured radial temperature profile in the plate is parabolic. The parabolic coefficient becomes Zero when the area averaged unburned gas velocity Ug at the exit of the burner plate matches with that of the laminar burning velocity S_L of the stabilized adiabatic planar flame. However, in practice it is difficult to adjust the unburned gas flow rate to represent the exact velocity where $U_g=S_L$. De Goey and co-workers circumvented this practical challenge by conducting multiple experiments by adjusting only the unburned gas velocity for a given initial condition and hence, the location of the flame with respect to burner was altered which results in change in net heat flux received by the burner plate and then by careful interpolation of the gas velocity towards a zero-heat flux provided the value of adiabatic laminar burning velocity of stabilized planar flames.

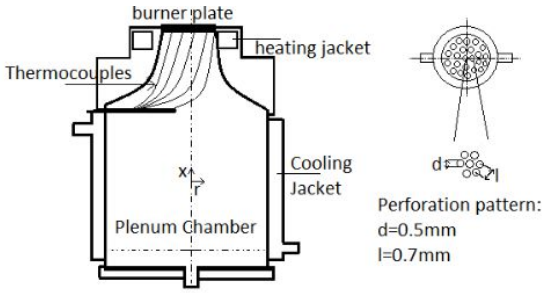

Figure.1. Left: Flat Flame burner with plenum chamber, cooling jacket and burner plate; Right: Top view of the burner showing the perforated pattern of the plate

The Heat flux was estimated from the measured radial temperature profile of the plate at a depth of 0.5mm from the top surface. The plate temperature profile provides valuable information on whether the burner plate is gaining or losing thermal energy from the flame.

One of the highlights of this rig was that it anchors planar, stretch-less, adiabatic flames. Care had to be taken to ensure that unburned gas velocity should be maintained to avoid flash-back or blow off conditions.

EXPERIMENTAL RIG AND PROCEDURE

As mentioned in Fig.2, the rig consisted of a flat flame burner having a custom drilled perforated burner plate, temperature-controlled burner head and plenum chamber. Inner surface of the burner was contoured to have a stream-lined flow. In the present work, premixed methane-air mixtures were primarily used. Digital Mass Flow Controllers (ALICAT) for Methane (0-10 SLPM) and for compressed dry air 0-50SLPM) were used to regulate at the desired flow rates. Methane and Air were allowed to mix in a Poly-Urethane (PU) Tubes (OD 8mm) having length of 4m. Residence time of gases inside this mixing tube was sufficient enough to attain a premixed combustible mixture before the plenum chamber.

Two SS meshes were used at the inlet section of plenum chamber to minimize the velocity fluctuations and straighten the premixed gas mixture inside the plenum chamber. Plenum chamber was fitted with cooling jacket to maintain the unburned gases at the initial temperature. The burner plate at the exit of the burner was made of brass. Its diameter was 31.5mm and its thickness was 2mm. It had 1499 through holes and 12 blind holes drilled in a staggered pattern (diameter of holes was 0.5mm and pitch between neighboring holes was 0.7mm, depth of blind holes was 1.5mm).

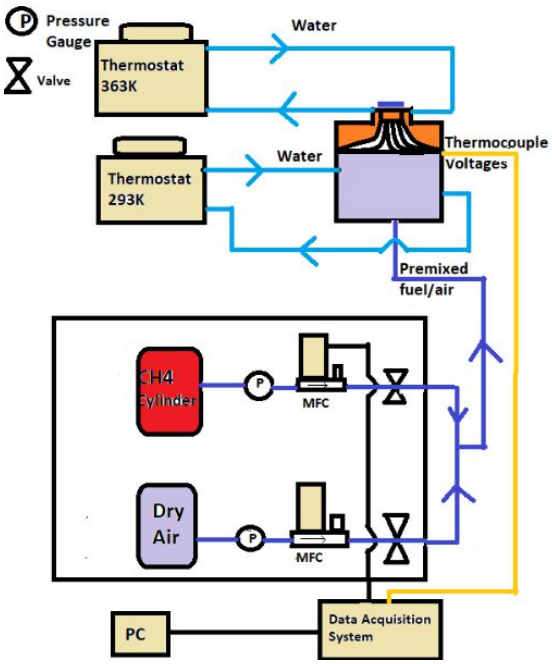

Figure.2. Experimental Lay-out of Flat flame burner

K-type thermocouples were attached into the blind holes which facilitate the plate temperature below the plate temperature measurements. The output voltage signal from K-type thermocouples was acquired in a Data Acquisition System (Agilent Make) at a sampling rate of 1000Hz. Burner plate was mounted in the burner head which had water heating jacket. Temperature controlled Water Circulation Bath (10L Capacity-Equitron Make) with a 0.5HP water pump was used to maintain temperature of the plate at 85^0C for all the studied conditions before anchoring the flame. Another cold-water circulation bath was used to maintain plenum chamber at desired unburned gas initial temperature. Till the entire flat flame burner rig attained the desired temperature, only air was used. Then methane was allowed to flow and a planar flame was anchored.

After anchoring the flame at a given flow rate, temperature of all thermocouples was recorded. Then the same exercise was repeated for more flow velocities. Recorded information was averaged and radial temperature profile of plate for each flow velocity was obtained.

Further processing was done using MATLAB to obtain adiabatic laminar burning velocity S_L.

The measured radial temperature profile of the burner plate at a given flow velocity was fitted with a parabolic function:

$$T_P(r) = T_C + Cr^2 \quad (1)$$

where T_P is the Temperature of the plate for radial direction, T_C is the Temperature at the center of the plate

$$C = -\frac{q}{4kh} \quad (2)$$

where C is the parabolic coefficient, k is the thermal conductivity of Brass and h is the thickness of the plate, q is the net heat flux received by the burner plate [5].

RESULTS ON LBV

Planar flame was anchored at the exit of the burner as explained in the previous sections. Experiments were conducted by varying equivalence ratios from 0.7-1.3 at 1 Bar and 300K. Fig. 3 shows the images of planar flames at different equivalence ratios. For a given gas mixture composition and thermodynamic conditions, the flame was anchored at different unburned gas velocities in order to vary the location from the burner plate and radial temperature profile for each flow velocity was measured. The velocity U_g is varied around the laminar burning velocity. For Φ=1, U_g was varied from 33cm/s up to 39cm/s. Fig. 4a) shows the measured temperature profile and the respective parabolic fit.

a)

b)

c)

Figure. 3. Flat flame images for various equivalence ratios; a) Φ=0.8, b) Φ=1.0, c) Φ=1.2

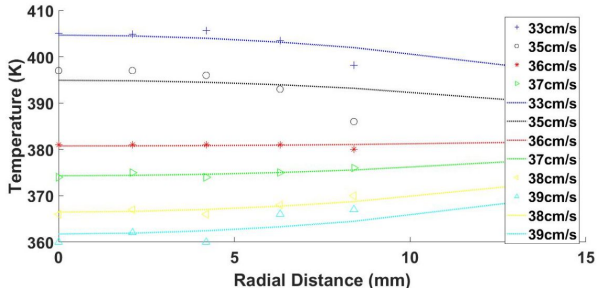

a)

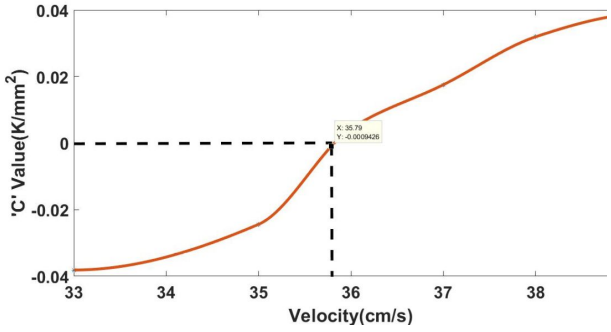

b)

Figure.4. (a) Parabolic Temperature profile in the burner plate at Φ=1; (b) Graph of 'C' Value corresponding to Φ=1

A parabolic curve was fitted as given in Figure 4(a). Resulting parabolic Coefficient *C* Values were plotted and interpolation was performed to obtain unburned gas velocity at zero heat flux as shown in Fig. 4(b). Fig. 4(b) shows that LBV of premixed methane air mixture at stoichiometric condition, 1 Bar and 300K is 35.7 cm/s.

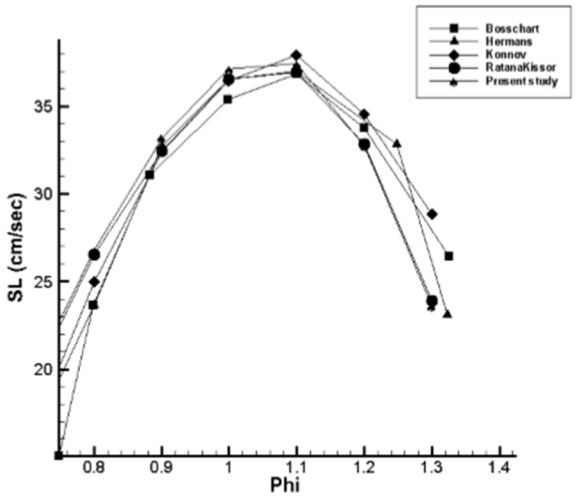

Figure 5. Variation of LBV of premixed methane air mixture with Φ at 1 Bar and 300K

Fig. 5 shows the change in LBV with Φ at 1 Bar and 300K for premixed Methane Air Mixture. Observation from the Fig. 5 indicates that LBV of premixed methane-air mixture attains maximum value at Φ=1.1. Present studied conditions show good comparison with literature data and the deviation is within the experimental uncertainties.

UNCERTAINTY ANALYSIS

There are several causes for errors and uncertainties involved in the measurement of LBV. The location and accuracy of embedded thermocouples play an important role in the measured temperature distribution and the uncertainty in S_L. To reduce the uncertainty caused by the temperature measurements, a UV thermographic phosphor ZnO:Zn has to be used on the burner plate surface to measure and control the temperature distribution [8]. Uncertainty in S_L due to temperature measurement is obtained by :

$$\Delta S_L{}^{TC} = \frac{\sigma_C}{s} \qquad (4)$$

where σ_C is Parabolic coefficient uncertainty given by:

$$\sigma_C = \sqrt{\frac{\frac{1}{N-2}\Sigma_i(T_i - C.(r^2)_i - T_{center}}{\Sigma_i((r^2)_i - \overline{(r^2)})^2}} \qquad (5)$$

where N is the number of thermocouples attached to the plate, C is the Parabolic coefficient from the graph and *s* is the
sensitivity of parabolic coefficient obtained from Figure 3.b) and is given by:

$$s = \left.\frac{dC}{dV_g}\right|_{V_g = S_L} \qquad (6)$$

The final uncertainty yielded was ΔS_L=0.220044 cm/s [7] and in addition to the temperature measurement, flow velocity measurement using mass flow controllers (MFCs) was also one of the largest causes of S_L uncertainty measurement in heat flux burners given by:

$$\Delta\phi = \phi\sqrt{(\frac{\Delta F_F}{F_F})^2 + (\frac{\Delta F_O}{F_O})^2} \qquad (7)$$

for which Full Scale Reading error % of Air and Fuel Mass Flow Control is 1%.

As can be seen from Fig.6., typical uncertainty is within 1% for Φ=1. For other equivalence ratios the errors become larger, because the relative error of the MFCs increases when producing smaller flows. Additional uncertainties associated with the heat flux method stem from radiation, boundary conditions at the burner surface, flame locationcatalytic effect of the metal plate, flame instability and flow disturbance from the burner holes. Another uncertainty may be introduced from the flame-wall interaction as the flame is stabilized very close (1-2mm) to the burner surface. Some of
the fuel may disappear already at the burner surface due to H abstraction by radicals, oxidation and diffusion. The composition at the burner surface may be different from that of the unburned mixture, leading to a change in the flame chemistry and structure [9].

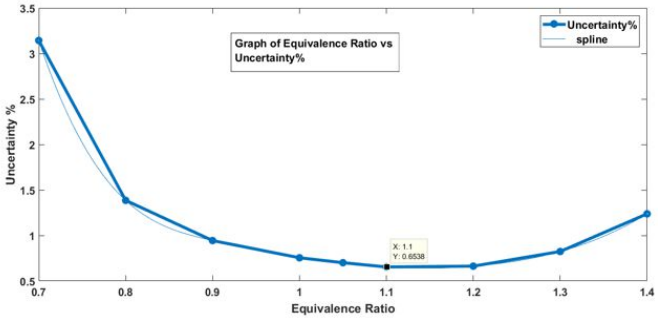

Figure. 6. Variation of Uncertainty with Φ

Estimation of Velocity Profiles using PIV

In the previous section, the commissioning of newly fabricated flat flame burner and testing its ability to anchor a planar premixed flame was discussed. Laminar Burning Velocity was measured for the anchored flames at different operating conditions and hence newly constructed burner was validated. Velocity field information at the exit of the burner is essential to compare it with the simulations. Velocity field at cold and reacting flow conditions may provide additional information on the presence of flame on the flow field. Hence, in the present work, velocity field at the exit of the burner was measured using Particle Image Velocimetry (PIV). It is a standard non- intrusive technique for measurement of velocity field. In this technique, the fluid flow is seeded with tracking particles that are illuminated by a thin laser sheet at least twice(double-pulsed) during a short interval of time '*dt*'. The Mie Scattered light from tracking particles were recorded by CCD Camera. After that each of the recorded images was divided into small interrogation windows to find the displacement of the particles within each window. The cross-correlation function was used to estimate the displacement of particles between two consecutive frames recorded with a time interval of *'dt'*. Layout of PIV rig is shown in Fig.14. PIV Experiments were conducted at NCCRD Center, IITM. It consists of Litron Bernoulli 145-15 PIV dual-pulsed Laser at a wavelength of 532nm was used to shine the tracking particles. The laser has a maximum output of 145 mJ at 532nm. Near field beam diameter was 5mm. Pulse width was 10ns. The repetition rate was 10 Hz. Mie scattered light from tracking particles was recorded using CCD Camera (PCO Pixelfly, 14-bit) with a resolution of 1.4MP. Nikon Tokina Macro AT-X M100 PROD lens was used of f=100mm, f/2.8 was used for focusing the field of interest to the camera.

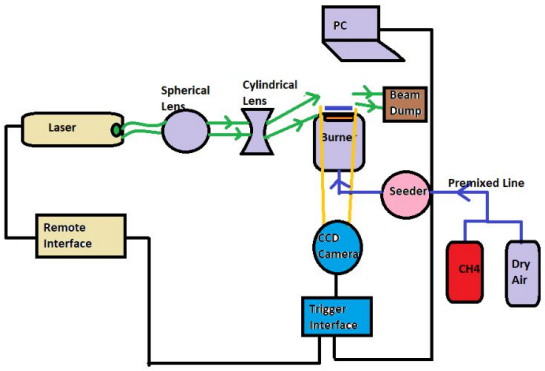

Figure 14. PIV Experimental Set up

A narrow band-pass filter with a range of 532±3 nm was attached to the lens. CamWare software was used to acquire images.

For the present measurements, both the lasers were operated at 80% of their maximum efficiency and along with 15% attenuation. Q Switch1 and 2 were kept at a delay of 200µs. Flash lamp 1 was triggered internally and 2nd was triggered externally through the CamWare software. For most of the operating conditions, the exposure time of camera was set at 400µs. The frequency of capturing was 6.78fps.

The time between the laser pulses(*dt*) or Flashlamp delay was controlled through remote interface of laser. After that laser beam was made to pass through a spherical lens and then a cylindrical lens(f=-10mm), producing a thin laser sheet approximately having a thickness of 1mm and a height of around 50mm. Laser sheet was aligned to pass through the burner axis and also it touched the top surface of the burner plate. Zirconium Dioxide (99.5% purity) particles having diameter less than 1µm was used as tracking particles. The properties of ZrO_2 are: density of 5.68g/cc, Melting Point of 2983K [10].

The time separation dt is given by the equation:

$$dt = \frac{\Delta x_i . q}{U} \qquad (8)$$

where Δx_i is the displacement vector considering
4 particles per interrogation window of size 32×32 pixels and 'q' is the magnification factor in terms of mm/pixel, U is the vector velocity of the flow
particles [11]. Only the sensor focusing on the area of interest, 31.5mm×22.5mm centered about the origin was enabled during recording and the image captured had a resolution of 1392×992 pixels resulting in a magnification of 44.25 pixels per mm.

Fig. 15 Set up image of PIV at NCCRD, IITM

Post-Processing of Mie Scattering Images

The post-processing was done with the help of commercial DaVis 8.4 Software. The image pre-processing steps begins with application of 3×3 Gaussian Smoothing Linear Filter. It was followed by "particle intensity normalization" operation. Then, Velocity Vector was Calculated using cross-correlation function via FFT transformation and Symmetric shift (both frames) was carried out for deformed interrogation windows. Finally, Multi-pass postprocessing was done by applying median filter. It was useful to remove and replace spurious vectors [12].

In the present work, deformed window size of 32×32 pixels along with multi-pass (constant size) with a Gaussian weighting factor 1:1 was used to calculate the velocity field. The overlap parameter defines the overlap between two interrogation windows next to each other. The larger the overlap, the larger the density of vectors calculated in the result. 50% Overlap was done with 5 iteration passes to effectively eliminate correlation errors [13]. The resolution of velocity vectors is around 0.364mm (16 pixels).

Cold flow field

Initially flow field at cold or ambient conditions was measured with only atmospheric air. By keeping a calibration plate at the plane and field of interest, camera was focused towards it and imaged. This serves as a calibration image for converting pixels into physical distance. Then air impregnated with ZrO_2 particles after it was regulated through digital mass flow controller using a seeding particle generator. Recorded images were post-processed following the steps presented in the earlier sections. Fig. 16 shows the planar velocity contour for an unburned gas velocity of 35cm/s at 1 bar and 295K without anchoring the flame. It clearly shows the presence of multiple jets as it is expected because of perforation configuration in the burner plate. In Fig. 17, the profile shows the magnitude of axial velocities in the radial directions at two different axial distances. At 3mm away from the plate, the velocity field is not yet developed because of strong interaction of multipple jets for unburned gas velocity ranging from 25-40 cm/s. At 10mm away from the burner, magnitude of axial velocity becomes nearly constant and matches close to that of estimate average velocity for all studied conditions.

Q (slpm)	Velocity(cm/s)	dt (μs)
9.78	25	775
14.84	35	553
16.96	40	484

Table1. Cold flow conditions

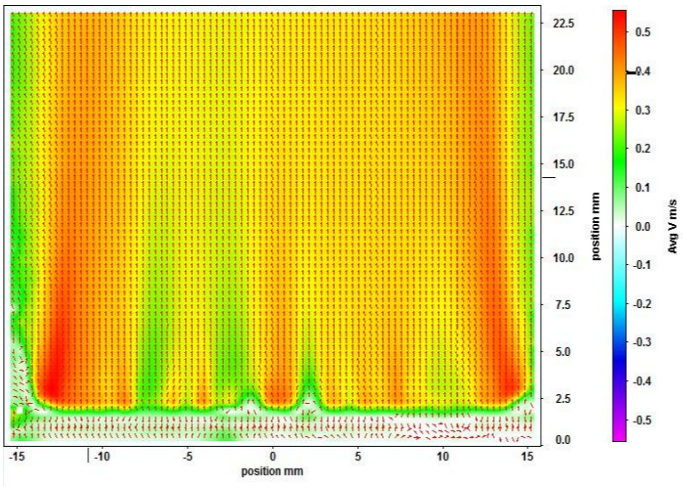

Fig. 16 Average Central planar velocity field above the burner plate for U=35cm/s at cold flow conditions measured using PIV

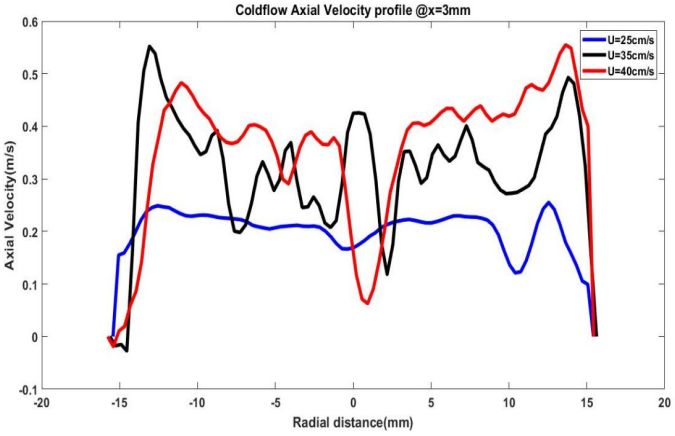

a)

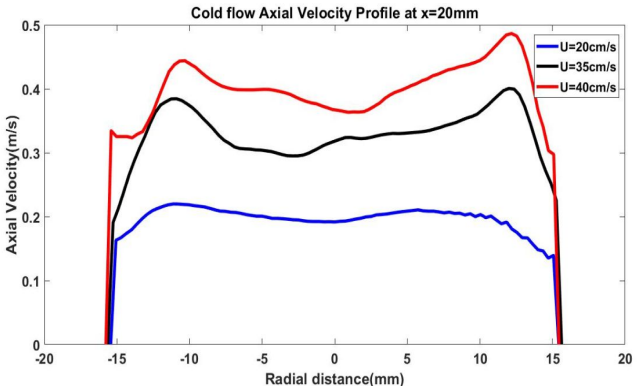

b)

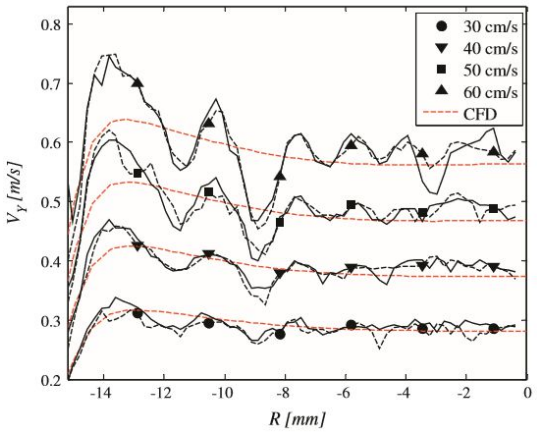

c)

Figure 17. Cold flow axial velocity profile comparison at a) x=3mm and b) x=20mm c) Literature data [14]

Observation of Fig. 17 shows that the radial distribution of axial velocity is not uniform near the burner exit and edge velocities are 19%, 54% and 34% greater than RMS Fluctuation velocities in 1-D area corresponding to the mean velocities of 25cm/s, 35cm/s and 40cm/s. Possible reason could be that the last round of holes in the burner plate does not have neighbors that might lead to slight increase in velocity closer to the edges. These fluctuations or non-uniformness are not certainly due to blind holes in the burner plate or due to the seeding. Most probably these fluctuations represent several jets issuing from the individual holes which interact with each other to form larger jets. Konnov., et. al [14] also reported similar observation in their experiments with a flat flame burner. As the axial height of the flow increased, the radial distribution becomes more uniform as shown in Fig. 17(b).

Axial Velocity profile of reacting flow

After completion of the experiments at cold flow conditions, velocity field was measured at reacting flow conditions. As the flame was closer to the burner plate, it was quite difficult to resolve the unburned gas velocity field upstream of reaction zone. Hence, burned gas velocity was resolved. The velocity field of burnt gas was equally important as it is closely related to the flame temperature distribution. For a given initial operating condition such as equivalence ratio, initial pressure and initial temperature, the flame was anchored with mean unburned gas velocity closer to that of laminar burning velocity measured with the same rig. Experiment was conducted for 6 different equivalence ratios of Φ=0.8 till 1.3 and the corresponding mean unburned gas velocities of premixed methane-air are mentioned in Table 2.

U (cm/s)	Φ	Q_{air} (slpm)	Q_f (slpm)	*dt* (μs)
25	0.8	9.781	0.821	100
30	0.9	11.62	1.09	100
35	1.0	13.43	1.411	100
40	1.1	15.207	1.757	100
35	1.2	13.18	1.661	100
26	1.3	9.71	1.32	100

Table2. Reacting flow conditions

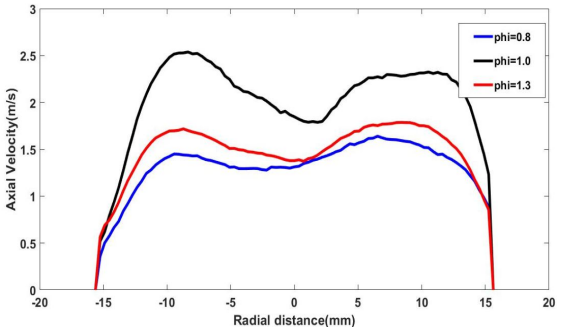

Fig. 18 Axial velocity profile for burnt gas at x=3mm

Fig. 18 shows the magnitude of the burnt gas velocities at x=3mm above the burner.

The effect of buoyancy on the axial velocity is shown in Fig. 19 for Φ=0.8,1.0,1.3 at r=0 by varying x. The acceleration of the burnt gas is clearly seen at 1.4mm above the burner plate. It can be seen that below x=1mm (i.e., in the flame zone), the results for V are unreliable because of the seeding slip, induced by the steep velocity increase in the flame zone [15].

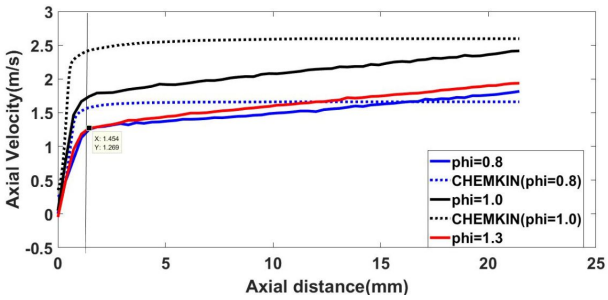

Fig. 19 Axial Velocity profile of the burnt gas as a function of x at r=0mm for Φ=0.8,1.0,1.3 compared with CHEMKIN simulations

Inorder to validate the experimental axial velocity profile along the height with respect to the burner plate, simulation was done for Φ=0.8 and Φ=1.0 using burner stabilised premixed laminar flame model in CHEMKIN. BURN flame code computes the velocity profiles using cold mass flow rates through burner and by solving energy equation. Thermodynamic and transport properties were taken from GRI 3.0 mechanism file. Prior to any calculations, the energy equation requires initial estimations of grid approximations and input variables. This is supplied with adaptive mesh points with maximum gradient and curvature set at 0.3. Values were given for the desired starting and ending axial positions. Velocities for premixed cold gas inlet were specified, compositions were provided with CH_4 as fuel and O_2 and N_2 as oxidisers with stable products as H_2O, CO_2 and N_2. Number of moles were substituted for each species. Using Gas-Energy Equation Problem type, Axial Velocity for Φ=0.8 and Φ=1.0 were simulated.

Radial Velocity profile for burnt gas

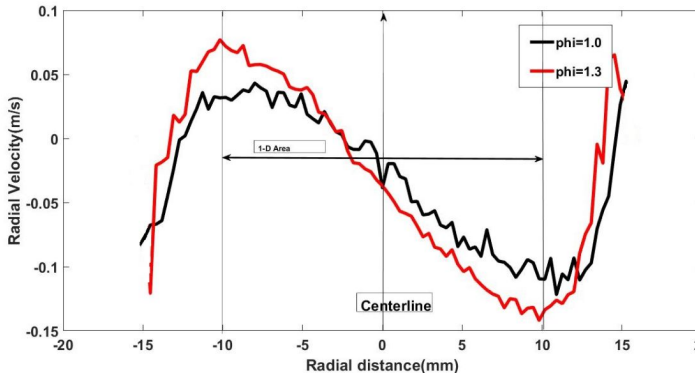

Fig. 20 Radial Velocity profile of burnt gas for Φ=1.0,1.3 at x=20mm

The radial velocity profile is shown in the Fig. 20 for Φ=1.0,1.3 at x=20mm. Fig. 20 clearly shows the linear relationship between the radial velocity and radius in the 1-D Area. The values of radial component of velocities is small as compared to its axial components and justifies that the anchored flame was one dimensional.

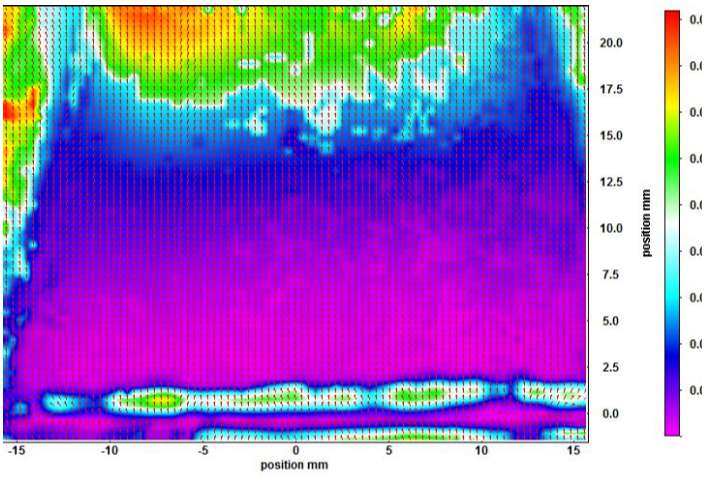

Fig. 21 Uncertainty Velocity field for Vy component(m/s) at Φ=0.8

Uncertainty analysis was done using Davis 8.4 for Vy component for Φ=0.8 and the magnitude is approximately 1cm/s up to 10.5mm above the burner plate and increases to 2cm/s till 17.5mm. There are various factors that cause errors and inaccuracies in the measurements.
The detection probability for a given ensemble of realizations of experimental parameters is defined to be probability, calculated for all realizations, of a single realization yielding a velocity measurement for which the detectability is larger than the pre-set threshold level. Monte Carlo simulation has to be done for the valid detection by making a comparison between U_m and U_{max} [16].

OH-PLIF Qualitative Measurements

The measurement of OH species in the planar flame was performed using non-intrusive laser diagnostic technique Planar Laser Induced Fluorescence (PLIF). In this paper, the PLIF rig to image OH Species, post-processing methods and qualitative measurements were presented. The quantitative measurements and its proper calibration with the help of UV-Absorption Spectroscopy technique is yet to be carried out. Its result will be presented in the future platforms.

PLIF Experimental setup

PLIF rig at NCCRD.IITM was used for the present measurements. The PLIF rig consists of a Nd: YAG Laser (Quantel Model *YG981E/IR-10*) which serves as a pump laser. It generates pulsed laser beam having diameter of 8mm at 532nm. The repetition rate was 10Hz and pulse width was 10ns. It was used to pump tunable dye laser (Quantel TDL+). In the present work, the desired wavelength to excite OH was 283.553nm which corresponds to the $Q_1(8)$ transition of OH denoted by $A^2\sum^+ (v'=1) \rightarrow X^2\prod (v'' =0)$ in the temperature range of 1500-2300K. Hence the dye cell in the dye laser was filled with Rhodamine 6G solution in ethanol. Laser beam at 532nm after passing through the dye laser emanates out at wavelength of 565.623nm. Then its frequency was doubled using a frequency doubling crystal, which outputs a UV laser beam at the required wavelength of 283.553nm. The pulse energy for all the studied conditions was maintained around 2.5mJ for line width of 0.7 cm^{-1}.
Then the cylindrical laser beam was made to thin sheet with a height of 20mm and a thickness of 1mm using sheet optics that consists of spherical lens and cylindrical lens. LIF emissions from the excited OH radicals were recorded using ICCD Camera (Princeton Instruments PI-Max3- 16-bit-1024×1024 pixels) equipped with UV Lens (Hamamatsu A4869, f=50mm, f/3.5) and a broadband OH filter (diameter 60mm) of range 280-310nm was used. ICCD Camera was positioned perpendicular to laser sheet and focused at the central plane of the flame.

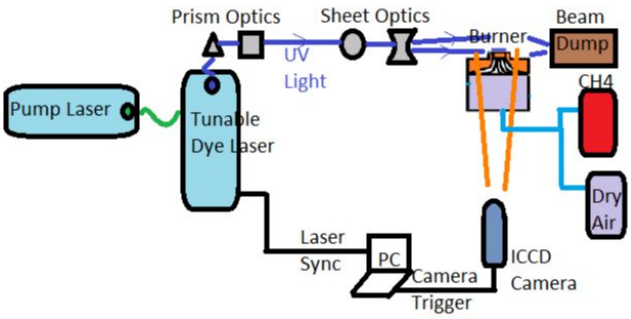

Figure 22. Experimental set up of OH-PLIF

The Laser was externally triggered and synchronized with ICCD Camera using Flowfield© software. In the present measurements, the ICCD Camera was operated at a gain of 50% which was sufficient enough to record emissions from OH species. After anchoring a steady flame, the OH intensity was recorded for a duration of 20s i.e., 200 images at 10Hz. During post-processing initial transient behavior could be observed in the recorded images, i. e, pixel intensity count changed from frame to frame before reaching a steady state, even though all parameters such as laser energy, power rating of burner held constant. Therefore, convergence test was performed for each experiment and it shows that a minimum of 100 images or 10 seconds of intensity data was required to

obtain accurate information for the present studied conditions [17].

PLIF Image Post-processing

OH-PLIF experiment was done by setting constant flow rates for the mean gas velocities of 14.76cm/s, 18cm/s, 22cm/s, 26cm/s and varying equivalence ratios from 0.8-1.3. Emissions were recorded for duration of 20 seconds. The recorded images were post processed in the following manner. Initial step involved scaling of image field from pixels to physical distance using calibration image recorded only with a calibration plate and without flame. Then the images were resized to a regime of interest 60×60mm.

Next, averaging the images for a given measurement were done by applying moving average method to remove fluctuations in time. Then background image was subtracted from the averaged signal image.

RESULTS

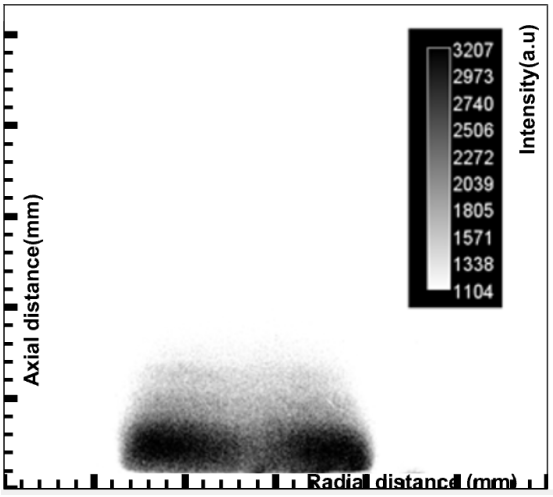

a)

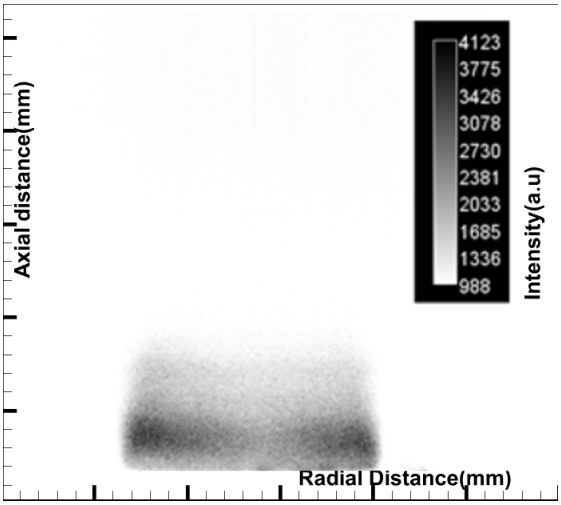

b)

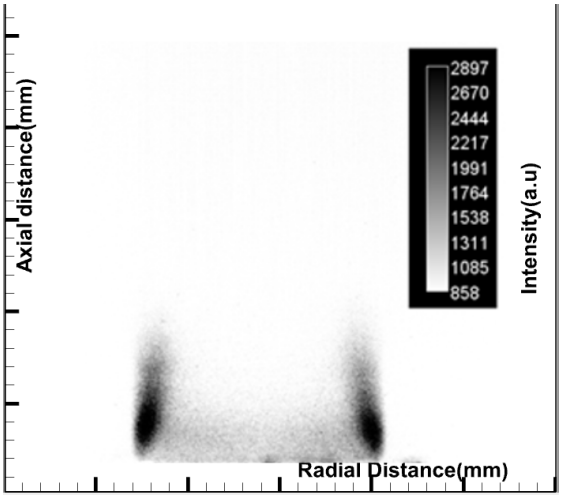

c)

Figure. 23 OH-PLIF images (60mm×52mm) for a) Φ=0.8 b) Φ=1.0 and c) Φ=1.3 for U=26cm/s

It can be observed that OH PLIF Intensity is almost constant throughout the burner plate in Fig. 23 a) and b) for Φ=0.8 and Φ=1.0 respectively. But the OH-intensity reduces at a greater magnitude at Φ=1.3. These variations in the OH Intensity for different equivalence ratios have to be investigated thoroughly and measurements in terms of OH-Mole fraction and Flame Temperature have to be quantified.

CONCLUSION

In this work, a new flat flame burner rig was designed following the literature and fabricated. It was tested using premixed methane air mixtures at different equivalence ratios, 1 Bar and 300K. Present measurements matched well with the literature data and hence the new burner was validated. After validation, 2D PIV experiments were conducted at both cold and reacting flow conditions. Measured velocity field measurements clearly showed the presence of multiple jets due to the perforated burner plate configuration at cold flow conditions. The measured axial mean velocity at a given axial distance matched closely with flow rates estimated from the digital flow meters. Burnt gas velocity was compared as well and it was compared with 1D simulations results obtained using burner stabilized flame model in CHEMKIN. PLIF measurements were attempted. OH intensity plots showed consistency within radius of 7.5mm and consistently bright luminosity closer to the flame edges were clearly observed. Similar observation was reported in literature too. Quantitative information on PLIF needs to be carried out yet. Hence, in the present work, a new flat flame burner was designed, fabricated and characterized.

ACKNOWLEDGEMENTS

We thank Department of Space for their generous funding in carrying out this research work. We sincerely thank Prof S.R Chakravarthy for allowing us to conduct experiments at NCCRD, IIT Madras. We also thank Mr. Shafeer, NCCRD, IITM for his contribution throughout the measurements.

REFERENCES

1. Arnold, A, et. al, 1996, “Quantitative measurements of OH Concentration fields by two-dimensional

laser-induced fluorescence", *Applied Physics B, 64, 579-583(1997)*

2. Zabarnick, S, Alspach D. A, 1991, "Absolute Concentration Measurements of Free Radicals in flames by Absorption Spectroscopy", *Report of Air Force Systems Command, Phillips Laboratory, US Govt.*

3. Hermanns, R, T, E., de Goey, L, P, H., 2007, "Laminar Burning Velocities of Methane-Hydrogen-Air Mixtures", Thesis, Eindhoven University of Technology, Netherlands

4. Botha, J, P., Spalding, D, B., 1954, "The laminar flame speed of propane/air mixtures with heat extraction from the flame", *Proc. Roy. Soc. Lond. A, 255:71*

5. Bosschaart, K, J., de Goey, L, P, H., 2002, "Analysis of the Heat Flux Method for Measuring Burning Velocities", Thesis, Eindhoven University of Technology, Netherlands

6. Arjen Van Maaren,1994, "One Step Chemical reaction parameters for premixed laminar flames*", Thesis, Eindhoven University of Technology*

7. Vladimir A. Alekseev et.al, 2016, "Experimental Uncertainties of the Heat Flux Method for Measuring Burning Velocities", *Combustion Science and Technology, 2016, VOL. 188, NO. 6, 853–894*

8. Li B, Linden J, Li ZS, Konnov AA, Alden M, de Goey LPH, "Accurate Measurements of laminar burning velocity using the heat flux method and thermographic phosphor technique", Proc Combust Inst 2011;33:939-46

9. Egolfopoulos, F, N., Kohse-Höinghaus, K., et. al., 2014, "Advances and challenges in laminar flame experiments and implications for combustion chemistry", *Progress in Energy and Combustion Science 43(2014) 36-6.*

10. Fang Chen, Hong Liu,2017, "Particle Image Velocimetry for combustion measurements: Applications and developments", *Chinese Journal of Aeronautics (2018)*

11. Adrian, R.J.,1997," Dynamic Ranges of velocity and spatial resolution of particle image velocimetry", *IOP Science, Meas. Sci. Technol. 8 (1997) 1393–1398*

12. Qian Xu, 2016, "Time Resolved Particle Image Velocimetry Measurements of the 3-D Single Mode Richtmyer-Meshkov Instability", *MS Thesis, The University of Arizona.*

13. Christof Heeger,2011," Flashback Investigations in a premixed swirl burner by high speed laser imaging', *Doktor-Ingenieurs Dissertation*, University of Darmstadt.

14. Konnov, A.A., et.al, 2013, "2-D effects in laminar premixed flames stabilized on a flat flame burner", *Experimental Thermal and Fluid Science 47 (2013) 213–223.*

15. Richard D Keane, Ronald J Adrian, 1991, "Optimization of particle image velocimeters: II. Multiple pulsed systems*", IOP Science, Meas. Sci. Technol. 2 (1991) 963-974.*

16. Stephen Hammack et.al,2014," Continuous hydroxyl radical planar laser imaging at 50kHz repetition rate", *APPLIED OPTICS / Vol. 53, No. 23 / 10 August 2014*